Electronic Supplementary Material (ESI) for Chemical Science.
This journal is © The Royal Society of Chemistry 2019

# Improving the reactivity of hydrazine-bearing MRI probes for in vivo imaging of lung fibrogenesis

## Supplementary Information

Eman A. Akam,[a,b,c] Eric Abston,[a,d,e] Nicholas J. Rotile,[a,b] Hannah R. Slattery, [a,b] Iris Y. Zhou,[a,b,c] Michael Lanuti,[c,e] and Peter Caravan*[a,b,c]

[a] *Martinos Center for Biomedical Imaging, Massachusetts General Hospital (MGH)*
[b] *The Institute for Innovation in Imaging, MGH*
[c] *Harvard Medical School, Boston, USA*
[d] *Boston University School of Medicine: Pulmonary, Allergy, Sleep & Critical Care Medicine, Boston, USA, and*
[e] *The Division of Thoracic Surgery, MGH, Boston, USA*

## Table of Contents

# General experimental methods

***HPLC-MS:*** HPLC-MS purity analysis was carried out on an Agilent 1260 system (UV detection at 220, 254 and 280 nm) coupled to an Agilent Technologies 6130 Quadrupole MS system using the following methods:

Mobile Phases: A: $H_2O$ (+ 0.1% formic acid, v/v) B: $CH_3CN$ (+ 0.1% formic acid, v/v)
C: $NH_4OAc$ 10 mM in $H_2O$, D: 90% ACN, 10% solvent C

Method 1: Column: Phenomenex Luna, C18(2), 5µm, 100 × 2 mm column Flow rate: 0.7 mL $min^{-1}$:

| min | %A | %B |
|---|---|---|
| 0 | 95 | 5 |
| 3 | 5 | 95 |
| 4.5 | 5 | 95 |
| 5 | 95 | 5 |
| 7 | 95 | 5 |

Method 2: Column: Restek, UltraAqueous C18, 5µm 250×10 mm column. Flow rate: 1.0 mL $min^{-1}$:

| min | %A | %B |
|---|---|---|
| 0 | 95 | 5 |
| 2 | 20 | 80 |
| 8 | 5 | 95 |
| 9 | 95 | 5 |
| 10 | 95 | 5 |

Method 3: Column: Restek, UltraAqueous C18, 5µm 250×10 mm column. Flow rate: 0.7 mL $min^{-1}$:

| min | %C | %D |
|---|---|---|
| 0 | 95 | 5 |
| 0.5 | 95 | 5 |
| 6 | 5 | 95 |
| 7.5 | 5 | 95 |
| 8.5 | 95 | 5 |
| 10 | 95 | 5 |

***Flash chromatography:*** Large-scale reverse-phase purifications were carried out on a Teledyne ISCO Combiflash system with UV-Vis detection using the following methods:

Mobile Phases: A: $H_2O$ (+ 0.1% formic acid, v/v) B: $CH_3CN$ (+ 0.1% formic acid, v/v)
C: $H_2O$ buffered with 50 mM $NH_4OAc$, D: 90% CAN with 10% solvent C.

Method 4: Column: 50 g Ultra-aqueous gold, flow rate: 70 mL $min^{-1}$:

| Column volume | %A or C | %B or D |
|---|---|---|
| 0 | 95 | 5 |
| 3 | 95 | 5 |

| | | |
|---|---|---|
| 7 | 5 | 95 |
| 9 | 5 | 95 |
| 8 | 95 | 5 |
| 10 | 95 | 5 |

***Preparative HPLC:*** Preparative reversed-phase HPLC with UV detection at 220, 254 and 280 nm was performed using the following methods:

Mobile Phases: A: $H_2O$ (+ 0.1% FA, v/v) B: $CH_3CN$ (+ 0.1% FA, v/v)

Method 5: Column: Restek, UltraAqueous C18, 5µm 250×10 mm, UV detection at 220nm, flow rate: 11 mL/min

| min | %A | %B |
|---|---|---|
| 0 | 100 | 0 |
| 10 | 100 | 0 |
| 40 | 5 | 95 |
| 45 | 5 | 95 |
| 46 | 100 | 0 |
| 51 | 100 | 0 |

***HPLC-ICP-MS:*** HPLC-ICP-MS was carried out on an Agilent 1260 HPLC system coupled to an Agilent 8800-QQQ ICP-MS system using the following HPLC method:

Mobile Phases: A: $H_2O$ with 0.1% formic acid, (v/v) B: $CH_3CN$ with 0.1% formic acid, (v/v)
C: $H_2O$ buffered with 10 mM, $NH_4OAc$ D: 90% ACN, with 10% solvent C.

Method 6: Column: Restek, UltraAqueous C18, 5µm 250×10 mm column. Flow rate: 1 mL/min

| min | %C | %D |
|---|---|---|
| 0 | 100 | 0 |
| 2 | 100 | 0 |
| 14 | 35 | 65 |
| 14.5 | 5 | 95 |
| 16 | 5 | 95 |
| 18 | 95 | 5 |

***Reaction rates with LC-ICP-MS***

In addition to UV-Visible measurements, apparent (pseudo-first order) rates for reactions of Gd-Hyd and Gd-CHyd with 2-formyl pyridine were also determined using a HPLC with ICP-MS detection. Similar to the UV-Vis kinetics experiment, reactions were conducted in pH 7.40 phosphate-buffered saline under pseudo-first order conditions with 2-formylpyridine concentration of 1000 μM and gadolinium-containing probes at 23 μM. Concentrations of unreacted starting material and condensation products were determined at 15 min time intervals over 1.5 hours based on their relative integrations. The values were fit to a standard first order rate constant linear equation and the rate constant was extracted from the slope.

***Binding to porcine aorta***

Allysine-rich porcine aorta was purified as previously described.[1] Solution of Gd-Hyd or Gd-CHyd ranging from 0.05 to 1 mM were prepared in PBS (pH 7.40) and 500 μL aliquots were added to 25 mg portions of purified aorta. The aorta segments were then incubated at 37 °C for 72 hours. The aorta pieces were then washed twice with PBS (pH 7.40), placed in concentrated nitric acid overnight for digestion. The gadolinium content was then assessed by ICP-MS.

***Binding to BSA-Ald***

Introduction of aldehyde moieties on bovine serum albumin (BSA) to produce oxidized BSA (BSA-Ald) was carried out as previously described.[2] Protein purification, quantification, and quantification of aldehyde load was achieved by literature reported procedues.[1] Aliquots of a solution of BSA-Ald (200 μL, 36 mg/mL (54 μM in protein, 55 μM aldehyde) were treated with Gd-Hyd or Gd-CHyd at various concentrations (200-10 μM) at 37 °C for 72 hours and then longitudinal relaxation ($T_1$) were measured and the inverse was plotted against concentration to obtain relaxivity. Additional solution of Gd-Hyd or Gd-CHyd were measured in the presence or absence of BSA protein for comparison. The samples were then passed through an ultrafiltration filter (5,000 Da cut-off PLCC cellulosic membrane, 30 mins, 10,000 RPM) to separate the protein-bound probe from the unbound probe and the Gd content of the filtrate was determined using ICP-MS.

***Stability of compounds in human plasma***

A 16 μL aliquot of the Gd-Hyd (1.0 mM) was added to 500 μL of human plasma (Lampire Biological laboratories). The solution was then incubated for 3 h at 37 °C. Aliquots (50 μL) were removed at 1, 2 or 3 hours. Proteins were precipitated by the addition of 150 μL of methanol, and removed following centrifugation. The supernatant was then analyzed using HPLC-ICP-MS (method 6). No unchelated gadolinium was observed nor the appearance of any new Gd-containing species.

***MR imaging***

For all animals, pre-injection baseline images as well as post-injection images were acquired for comparison. Mice were imaged on a 4.7 Tesla MRI scanner (Bruker, Billerica MA) using a custom-built volume coil. Animals were anesthetized with 1–2% isoflurane and air/oxygen mixture to maintain constant respiration rate at 60 breaths/minute monitored by a small animal physiological monitoring system (SA Instruments Inc., Stony Brook NY). Animals were kept warm using heated air flowing to the bore of the instrument. The probe was delivered as a bolus via an indwelling tail vein catheter.

Images were acquired with the following sequences and parameters:

T1 weighted 3D Fast Low Angle Shot (FLASH): repetition time (TR) / echo time (TE) / flip angle (FA) = 10 ms/2.5 ms/12°; field of view (FOV) 48 x 24 x 24 $mm^3$; matrix = 150 x 75 x 75; spatial resolution = 320 µm (isotropic); one average; acquisition time = 56 sec

Rapid Acquisition with Relaxation Enhancement (RARE): TR/TE = 1500 ms/8 ms; RARE factor = 4; FOV = 32 x 32 mm; matrix = 192 x 192; In-plane resolution = 167 x 167µm; slice thickness = 1mm; 15 slices; 4 averages; acquisition time = 3 min 36 sec

T1 weighted 3D Ultra Short TE (UTE): TR/TE/FA = 8 ms/8.25 us/8°; 51360 spokes; FOV = 32 x 32 x 32 $mm^3$; matrix 128 X 128 x 128; spatial resolution = 250 µm (isotropic); one average; acquisition time = 6 min 51 sec

# Supplementary figures and tables

***NMR spectra of Gd-CHyd intermediates:***

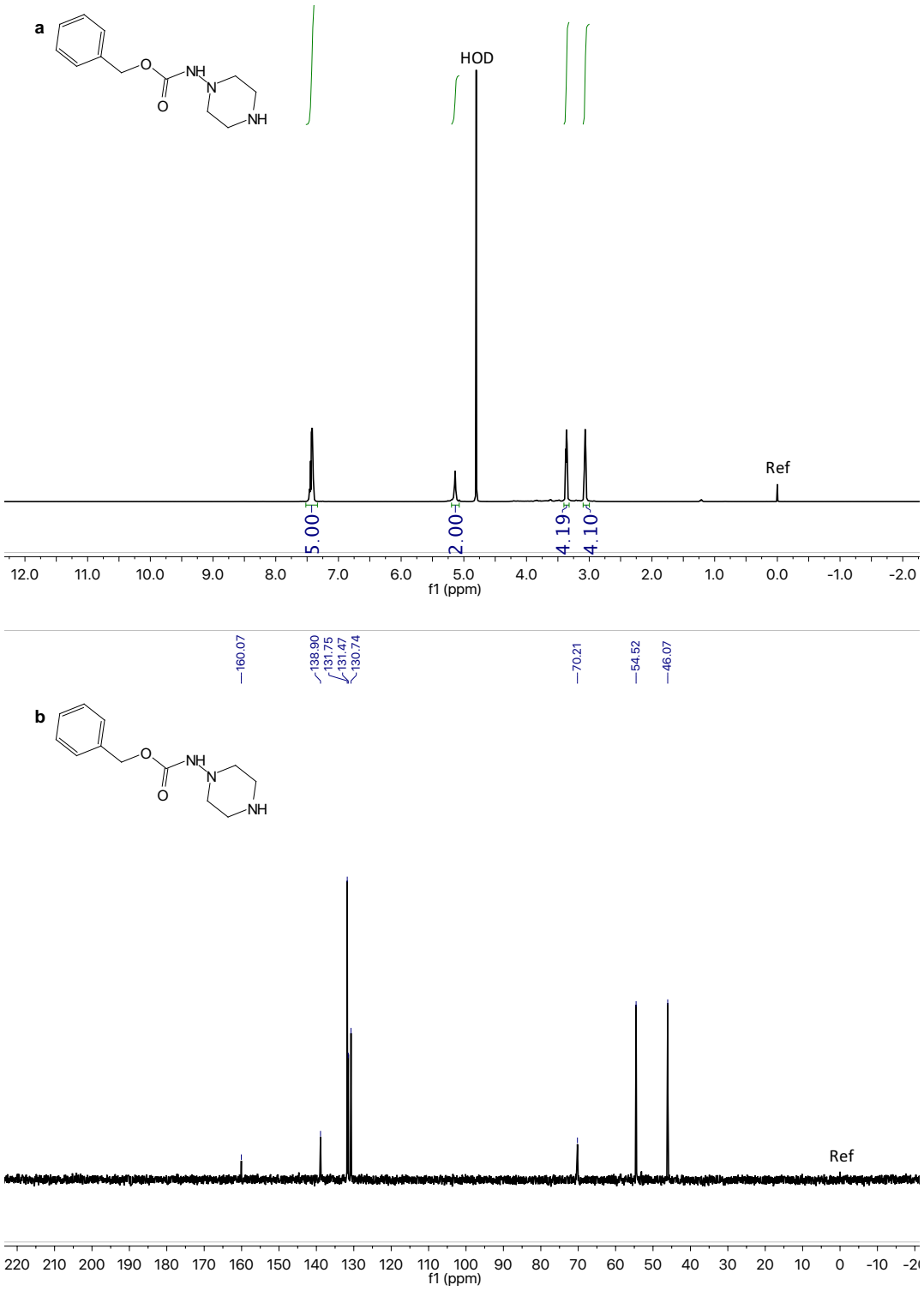


Fig S 1: $^{1}H$ (a) and $^{13}C$(b) NMR spectra of compound 1 (Main text Scheme 1) in $D_2O$. Residual solvent peak is marked (HOD) as well as the internal reference (Ref) 3-(Trimethylsilyl)propoionic-2,2,3,3-acid $d_4$ set to zero ppm.

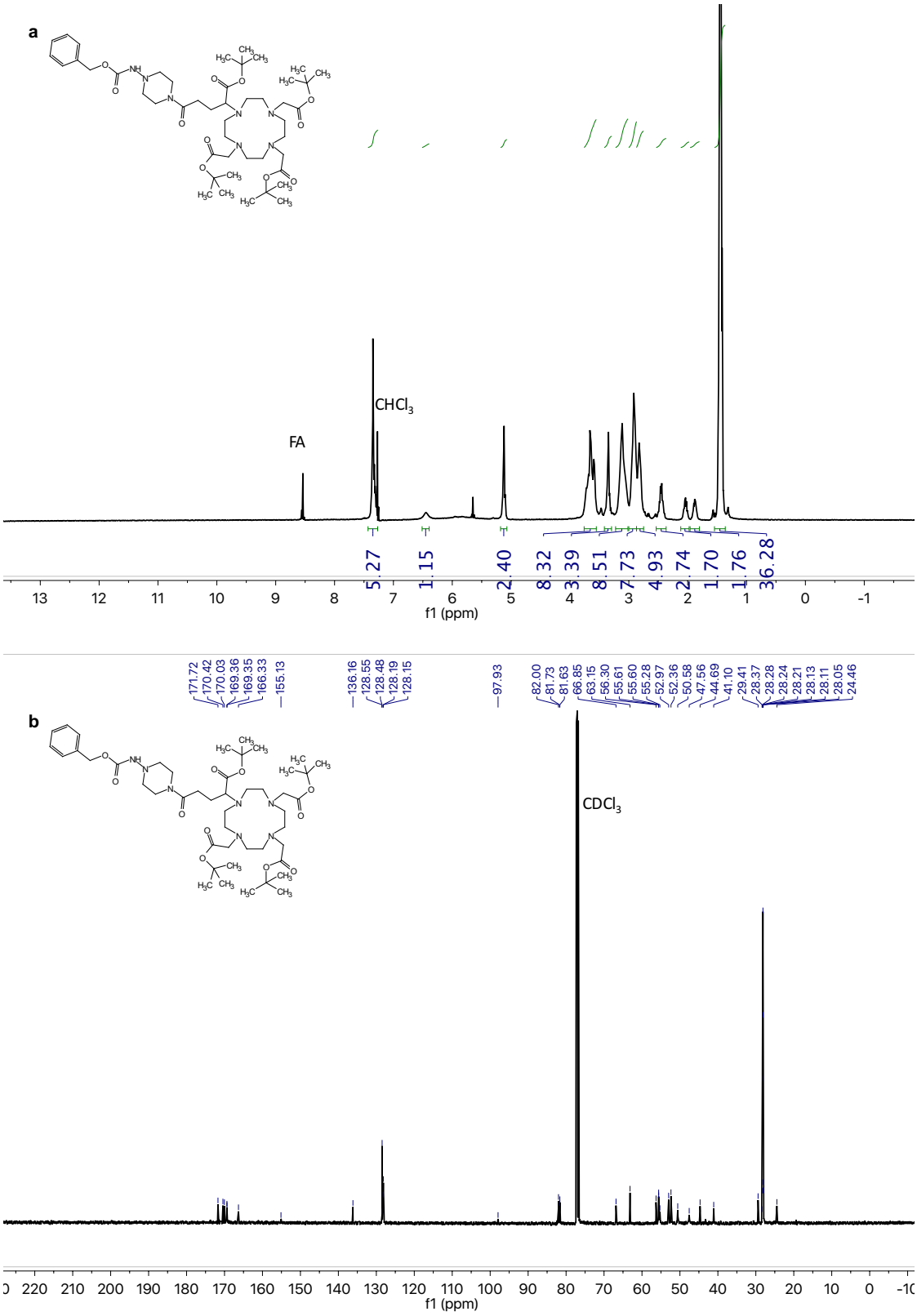


Fig S 2: $^{1}H$ (a) and $^{13}C$(b) NMR spectra of compound 1 (main text Scheme 2) in $CDCl_3$. Residual solvent peak is marked (HOD) as well as residual formic acid buffer (FA) used in the purification.

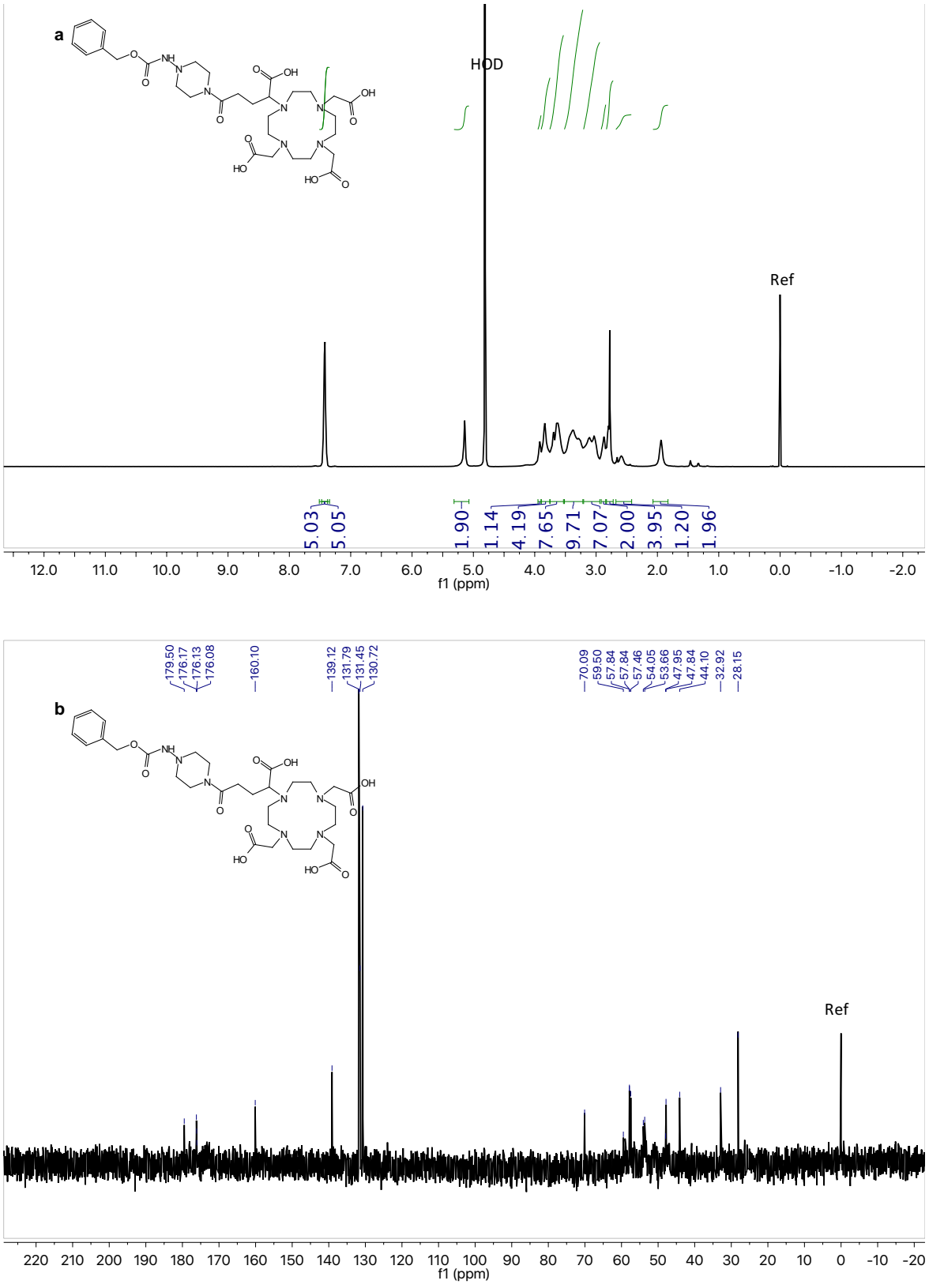


Fig S 3: $^{1}H$ (a) and $^{13}C$(b) NMR spectra of compound 3 (main text Scheme 1) in $D_2O$. Residual solvent peak is marked (HOD) as well as the internal reference (Ref) 3-(Trimethylsilyl)propoionic-2,2,3,3-acid $d_4$ set to zero ppm.

***Assessment of purity and reactivity by LC-ICP-MS:***

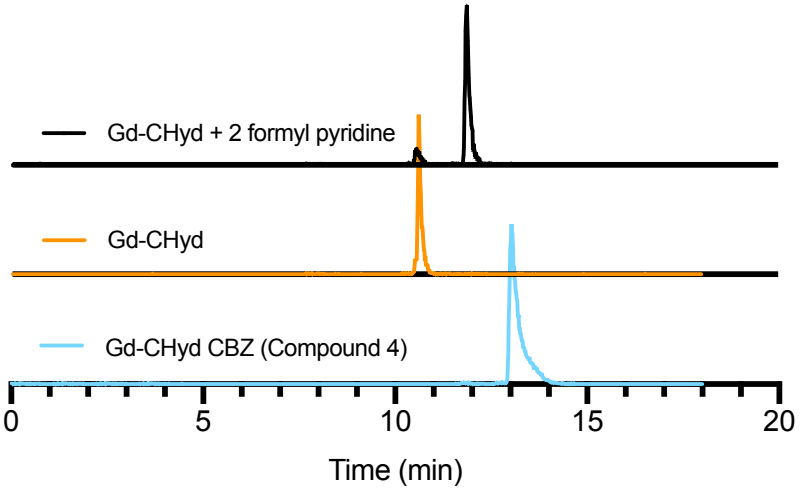


Fig S4: Assessment of purity of Gd-containing compounds using LC-ICP-MS with gadolinium detection using method 6 with A and B as solvents. Traces are shown for compound 4, precursor to Gd-CHyd, showing one Gd-containing species. After removal of CBZ group resulting in Gd-CHyd, the hydrazine is now reactive with the aldehyde 2-formyl pyridine as shown. The y-axes in the traces are of the normalized counts.

***Reaction rates using LC-ICP-MS:***

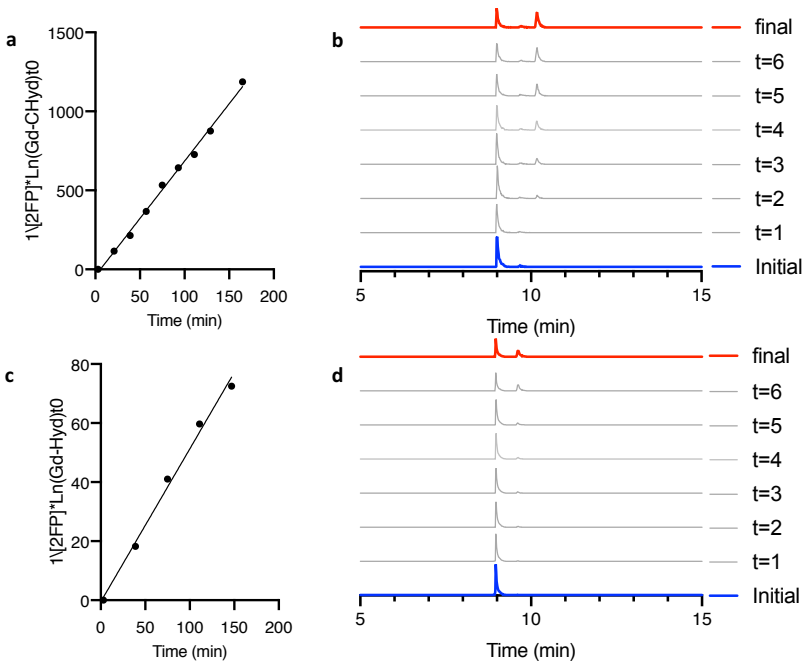


Fig S5: Determining the psudeo-first order rate constants for the reaction of Gd-Hyd and Gd-CHyd with 2-formyl pyridine (2-FP) using LC-ICP-MS with Gd detection. a & c) The linear fit obtained from relative integrations for Gd-CHyd or Gd-Hyd and their 2-FP condensation products b & d) LC-ICP-MS traces showing progression of the reaction of Gd- CHyd with 2FP with the initial unreacted probe shown in blue, and the final trace (after 150 minutes) shown in red.

| | $k_{obs}$, ($M^{-1}s^{-1}$) | Relative $k_{obs}$ |
|---|---|---|
| Gd-Hyd | 0.0086 | 1 |
| Gd-CHyd | 0.115 | 13 |

Table S1: The rate constant ($k_{obs}$) for the reaction Gd-CHyd and Gd-Hyd with 2-formyl pyridine under pseudo-first order conditions (pH 7.40 in PBS) as determined by LC-ICP-MS.

***Stability of compounds in human Plasma***

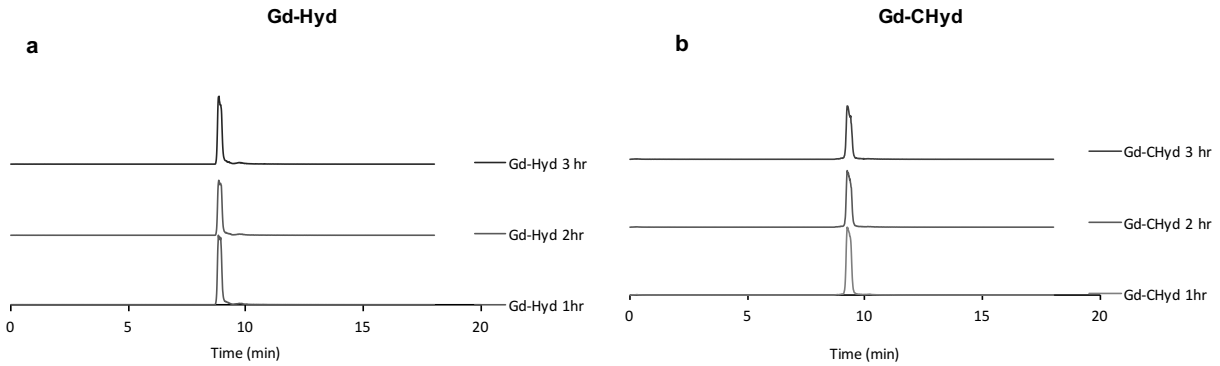


Fig S6: HPLC-ICP-MS traces detecting gadolinium containing species for a) Gd-Hyd and b) Gd-CHyd incubated with human plasma. There is no apparent de-chelation or formation of Gd-containing metabolites after incubation in plasma.

***Confirmation of protein binding of probes to aldehyde-rich BSA-Ald:***

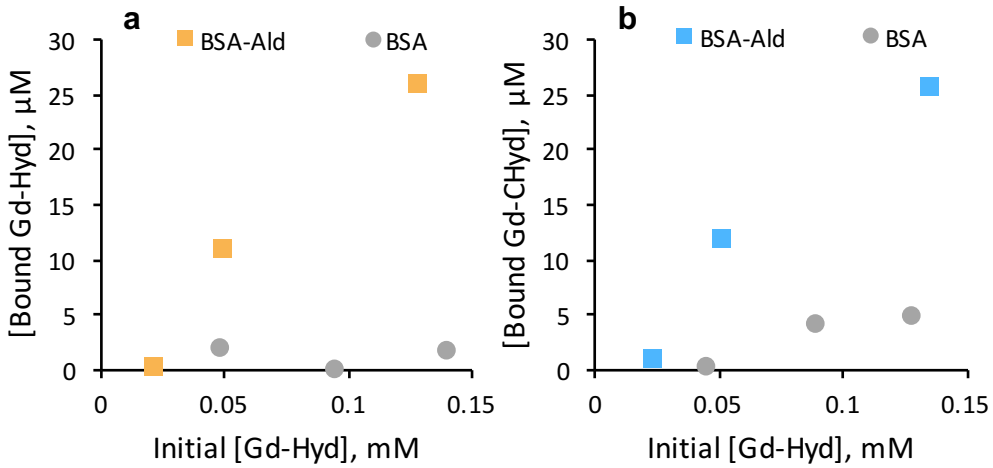


Fig S 7: The concertation of protein-bound Gd-Hyd (a) or Gd-CHyd (b) incubated with BSA-Ald or BSA as determined by ICP-MS. The samples passed through an ultrafiltration filter (5,000 Da cut-off)) to separate the protein-bound probe from the unbound probe. The Gd content of the filtrate was determined using ICP-MS and the amount bound in determined from the initial concentration of probe. While there is a concentration-dependent increase in binding of both Gd-Hyd and Gd-CHyd to BSA-Ald, minimal amounts of probe binds to unmodified BSA.

***MR imaging***

## Segmentation of lung parenchyma and defining regions of Interest (ROIs)

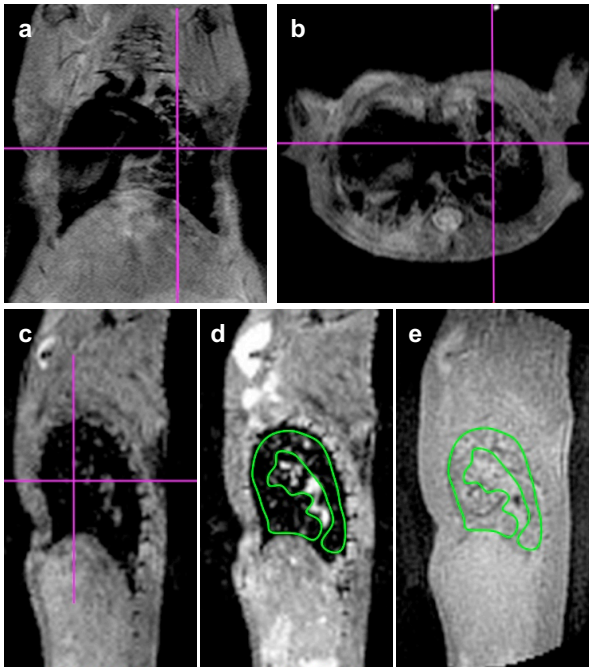


Fig S8: Example coronal (a) and axial (b) RARE MR images and 3D FLASH sequence pre (c) and post probe (d) injection. The RARE sequence is a black blood sequence that shows the myocardium, liver, and large airways against a black background. The enhanced regions on the post injection 3D FLASH image show large blood vessels and the heart. Images a-d are used to segment the lung and create regions of interest (ROIs, shown in green) that exclude airways and large vessels. The ROIs drawn on the 3D FLASH images are then copied onto the high-resolution UTE sequence (e) used for CNR quantification. Location of the various slices relative to each other are denoted by the magenta lines.

**Dynamic MRI showing biodistributions and clearance of Gd-CHyd**

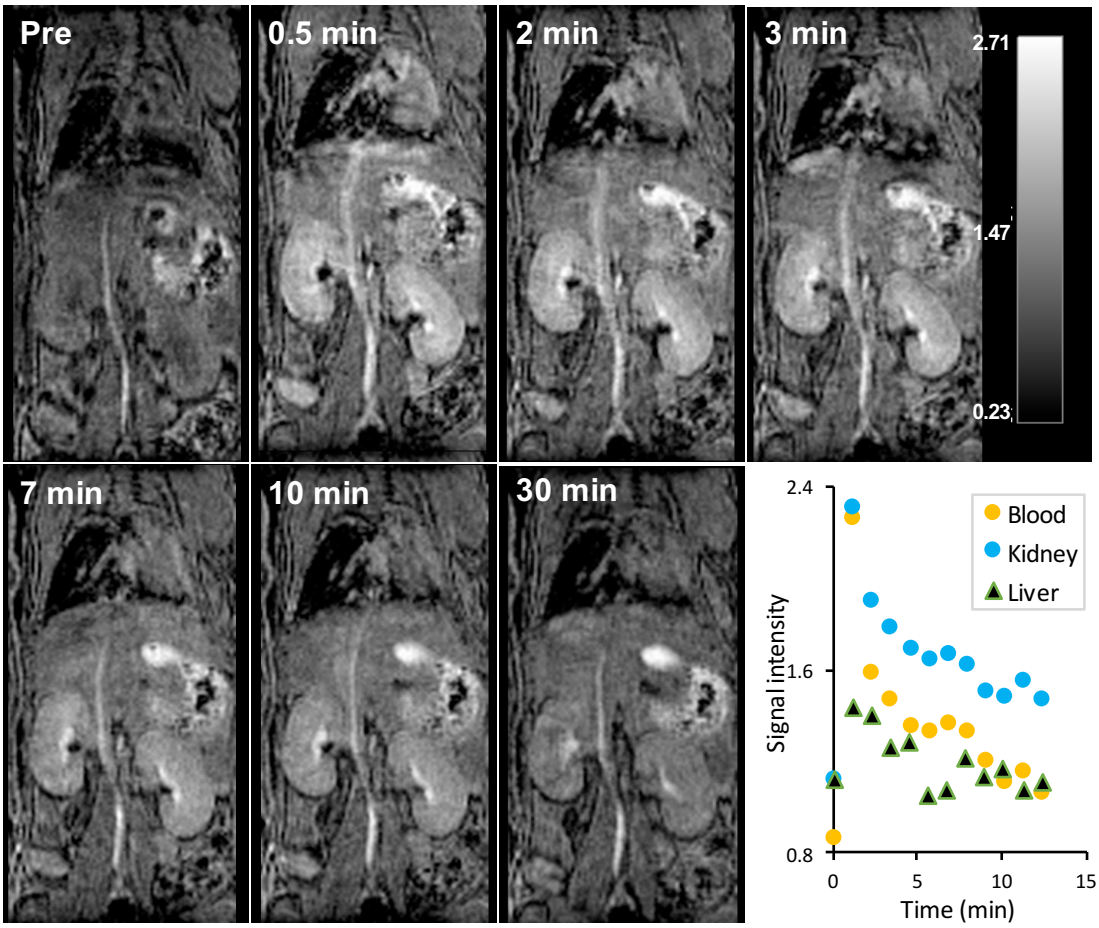


Fig S9: Representative time-dependent coronal 3D-FLASH MR images of a naïve mouse before and at several time points after injection with Gd-CHyd. In the field of view at this slice plane, the kidneys, part of the liver, the heart, and the stomach are all visible. Immediately following injection, the signal is enhanced in all tissue and clears rapidly with time. The clearance of the probe from the blood is followed by determining the signal in the heart (blood pool) and fitting the data to a monoexponential function. Quantification of the time dependent change in signal intensity in the blood, kidney and liver is shown on the graph in the bottom right. Note that the liver enhances slightly with first-blood pass but the signal rapidly return to baseline before the first time point at which MR signal in the lungs is quantified.

## Time-based quantification of Gd-CHyd MR signal in BM and naïve mice

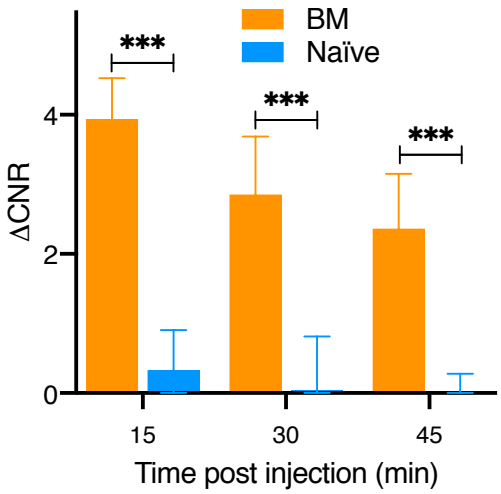


Fig S10: Comparison of the ΔCNR values in the lungs of bleomycin-injured animals or naïve animals at 15, 30 or 45 minutes post injection. ***p<0.001, t-test.

***Tissue analysis/biodistributions***

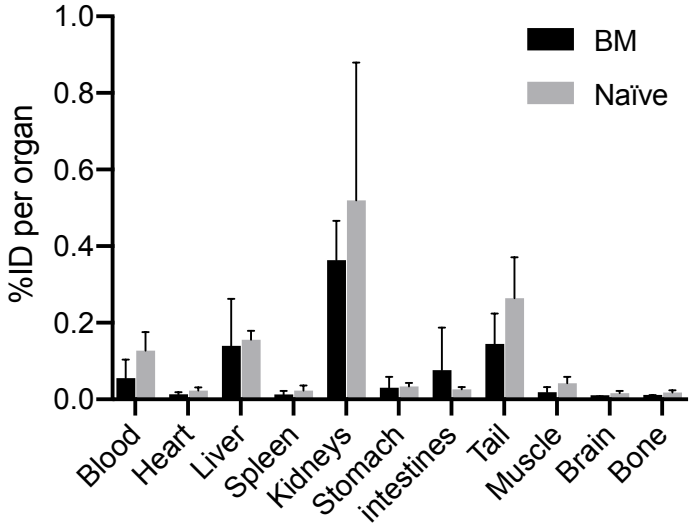


Fig S11: The gadolinium content in various tissues and organs of naïve or bleomycin-injured (BM) mice 75 minutes after injection of Gd-CHyd reported as the percent of the injected dose per organ. None of the differences between the two cohorts are statistically significant. Even at 75 minutes post injection most of the injected dose (>98%) has been eliminated from the body.

***References:***


1. H. H. Chen, P. A. Waghorn, L. Wei, L. F. Tapias, D. T. Schühle, N. J. Rotile, C. M. Jones, R. J. Looby, G. Zhao, J. M. Elliott, C. K. Probst, M. Mino-Kenudson, G. Y. Lauwers, A. M. Tager, K. K. Tanabe, M. Lanuti, B. C. Fuchs and P. Caravan, *JCI Insight*, 2017, **2**, e91506.
2. R. L. Levine, D. Garland, C. N. Oliver, A. Amici, I. Climent, A. G. Lenz, B. W. Ahn, S. Shaltiel and E. R. Stadtman, *Methods Enzymol*, 1990, **186**, 464-478.